INTERNATIONAL JOURNAL OF AUTOMOTIVE AND MECHANICAL ENGINEERING
ISSN: 2229-8649 e-ISSN: 2180-1606
VOLUME 23, ISSUE 3, 2026, 13738 - 13755
DOI: https://doi.org/10.15282/ijame.23.3.2026.1.1037

RESEARCH ARTICLE

Adaptive cruise control based on fuzzy logic for collision avoidance in autonomous vehicles

J.C. Suárez-Calderón*, I. Rocha-Gómez, O. Susarrey-Huerta, D. Desiderio-Maya

Instituto Politécnico Nacional, SEPI-ESIME-Zacatenco, Av. IPN S/N, Ed 5, 3-r piso, Ciudad de México, 07738, México

Abstract - Intelligent adaptive cruise control (IACC) systems have become a key technology for enhancing the safety and reliability of autonomous vehicles operating in dynamic traffic environments. This study proposes a fuzzy logic-based IACC architecture for collision avoidance that integrates longitudinal speed control, lateral steering control, obstacle detection, safety distance assessment, rollover prevention, and emergency braking into a unified decision-making framework. Given the high cost and complexity associated with full-scale vehicle experiments, the proposed system was implemented and validated within a MATLAB®/Simulink® environment, utilizing a dynamic model based on the real-world characteristics of a commercial passenger vehicle. The controller continuously estimates the distance to surrounding obstacles, assesses the vehicle's dynamic state, and autonomously selects the safest maneuver—coordinating lane-change and emergency braking actions while accounting for vehicle stability and passenger comfort. Three representative driving scenarios, featuring obstacles of varying sizes and positions, were designed to evaluate the controller under realistic operating conditions. Simulation results demonstrated a 99.9% success rate in collision avoidance, smooth trajectory tracking, stable speed regulation, effective rollover prevention via lateral acceleration monitoring, and reliable emergency braking in critical situations. These results demonstrate that the proposed fuzzy logic-based IACC architecture offers a robust and effective solution for autonomous collision avoidance by integrating multiple safety-oriented control strategies into a single intelligent framework. Furthermore, the proposed approach provides a promising foundation for future experimental validation and real-world implementation in autonomous vehicles.

Article History
Received : 14 February 2024
Revised : 6 March 2025
Accepted : 15 June 2026
Published : 21 September 2026

Keywords
Autonomous vehicle
Collision avoidance
Fuzzy control
Intelligent Adaptive Cruise Control
Safety control

1. Introduction

In recent years, the automotive industry has focused on developing technologies that increase safety, comfort, and efficiency while driving [1]. In this context, advanced driver assistance systems (ADAS) have been among the most significant innovations, incorporating functions designed to reduce human intervention and improve vehicle responses to risky situations [2]. Among these technologies, adaptive cruise control (ACC) has become a fundamental tool for automatically regulating vehicle speed and maintaining a safe distance from the vehicle ahead. Modern ADAS typically integrate ACC with warning, assistance, and collision prevention functions, allowing the vehicle to detect obstacles, assess risk conditions, and execute actions such as speed reduction or emergency braking. Several studies have demonstrated that ACC systems improve road safety and traffic efficiency by reducing sudden braking and the likelihood of rear-end collisions. Furthermore, the incorporation of multistate stochastic models has improved the adaptability of ACC systems to real-world traffic conditions [3]. This evolution has led to the development of fuzzy adaptive distance control (AFDC), which enhances the robustness and adaptability of conventional ACC strategies [4]. Cooperative adaptive cruise control (CACC) further extends these capabilities through vehicle-to-vehicle communication, thus improving traffic flow and string stability[5]- [6]. Recent studies have also introduced hierarchical ACC architectures that integrate fuzzy decision-making with multi-objective model predictive control (MPC), enabling simultaneous optimization of safety, ride comfort, and fuel economy under different driving conditions [7]. In addition, adaptive vehicle-following strategies based on variable-time headway models and MPC have further improved the dynamic adjustment of intervehicle spacing according to traffic conditions [8].

As the level of automation increases, autonomous vehicles require control strategies that can operate in dynamic, uncertain, and highly nonlinear environments. These systems must integrate environmental perception, obstacle detection, trajectory planning, decision-making, and maneuvering execution to ensure safe and reliable operation under diverse driving conditions [9]. In this context, fuzzy logic has become one of the most widely used intelligent control techniques because it can represent expert knowledge through linguistic rules and effectively manage uncertainty without requiring accurate mathematical models [10]. Consequently, fuzzy-based controllers have been widely adopted for vehicle control, collision avoidance, and autonomous navigation applications. The recent literature shows that fuzzy logic has evolved from basic speed control applications to hybrid architectures aimed at trajectory tracking, obstacle avoidance, and autonomous decision-making. A simplified decomposed fuzzy PID (SDFPID) controller was previously proposed to regulate the longitudinal speed of autonomous vehicles and was validated through CARSIM–MATLAB/Simulink co-simulation, providing a more stable response than conventional PID controllers [11]. Similarly, recent reviews indicate that fuzzy-PID and fuzzy-MPC controllers are promising alternatives for improving the adaptability of ACC systems under varying traffic conditions [12].

***CORRESPONDING AUTHOR | J.C. Suárez-Calderón**| ✉ jcarlos.suarez@live.com
© 2026 The Authors. Published by Universiti Malaysia Pahang Al-Sultan Abdullah Press. This is an open access article under the CC BY-NC 4.0 license

In trajectory tracking applications, fuzzy logic is frequently combined with MPC to improve vehicle stability during complex maneuvers [13]. More recently, Takagi–Sugeno fuzzy models integrated with MPC have demonstrated effective collision avoidance capabilities while reducing computational complexity and maintaining vehicle stability in dynamic environments, highlighting their suitability for autonomous driving applications [14]. Other researchers have optimized fuzzy controllers using evolutionary algorithms to reduce tracking errors and minimize the dependence on expert-defined membership functions [15]. Hybrid adaptive neuro-fuzzy inference systems (ANFISs) and neuro-fuzzy architectures have also demonstrated improved adaptability and robustness under dynamic driving conditions [16] –[17]. Fuzzy logic also offers advantages over conventional controllers in terms of lateral control. A fuzzy controller was compared with a PID controller in an autonomous vehicle equipped with an improved swerve drive system and demonstrated a reduction in overshoot and steady-state error [18]. Hybrid approaches combining terminal sliding mode control, radial basis function (RBF) neural networks, and fuzzy logic have improved lateral tracking performance and reduced chattering during lane-change maneuvers [19]. Furthermore, Type-2 fuzzy logic provides a smoother and more robust response to uncertainties than Type-1 fuzzy logic [20]. Moreover, Type-2 fuzzy logic controllers with Sugeno inference have demonstrated smoother responses and lower trajectory errors than conventional PID controllers under uncertain driving conditions [21]. Fuzzy logic has also been extensively applied to lane changing, path planning, and obstacle avoidance maneuvers. Intelligent navigation systems that integrate light detection and measurement (LiDAR), radar, GPS, cameras, and fuzzy decision-making have demonstrated improved environmental perception and autonomous navigation in dynamic traffic scenarios [22]. Hybrid approaches combining fuzzy logic with neural networks and environmental sensors have also enabled autonomous vehicles to determine whether an obstacle should be avoided or whether emergency braking is the most appropriate response [23]. Recently, integrated planning and control strategies based on improved artificial potential fields (APF) and fuzzy model predictive control (Fuzzy-MPC) have demonstrated enhanced obstacle avoidance performance while maintaining vehicle stability and tracking accuracy during emergency maneuvers, highlighting the effectiveness of combining intelligent path planning with advanced control algorithms [24]. Beyond direct vehicle control, complementary applications have also strengthened autonomous driving systems. Probabilistic trajectory prediction based on fuzzy logic has improved decision-making in complex traffic scenarios [25]. Furthermore, the detection and mitigation of denial-of-service attacks using fuzzy logic have shown that this technique can contribute to the cybersecurity of autonomous vehicles [26]. In addition, studies on autonomous vehicle platoons have highlighted the importance of integrating LiDAR, GPS, cameras, V2V communication, sensor fusion, and intelligent control to increase safety in cooperative driving environments [27].

Despite these advances, significant challenges remain in the implementation of ACC, CACC, and intelligent controllers. The main problems include sensor limitations, computational complexity, interactions with human-driven vehicles, real-time constraints, and the requirement for formal safety assurance mechanisms [28]-[29]. Although fuzzy logic has demonstrated considerable potential for handling uncertainty in autonomous driving, the design of membership functions and robust rule bases remains an important research challenge [30]. A review of the literature reveals that most studies have focused on solving specific problems in isolation, such as longitudinal control, lateral control, trajectory tracking, route planning, and obstacle avoidance. However, research integrating these functions into a unified intelligent adaptive cruise control architecture capable of combining perception, dynamic vehicle assessment, and real-time decision-making remains limited. In this context, this study proposes a fuzzy logic-based intelligent adaptive cruise control system for collision prevention in autonomous vehicles. The proposed system estimates the distance to obstacles, evaluates the dynamic conditions of the vehicle, and selects the most appropriate control action in risky situations. Unlike approaches that focus exclusively on longitudinal or lateral control, the proposed system coordinates decision-making between lane changing and emergency braking, prioritizing vehicle safety, maneuvering stability, and passenger comfort.

2. Materials and Methods

2.1 Problem Formulation

Several studies have focused on ACC systems to reduce collisions and optimize traffic flow efficiency. However, the factors inherent in human behavior remain a crucial challenge because they introduce significant uncertainty into the operation of autonomous vehicles. Traditional ACC systems exhibit notable limitations in responding to unexpected situations, such as sudden braking due to the sudden appearance of obstacles, and often lack the ability to perform essential maneuvers, such as lane changes. We address these limitations by proposing an intelligent cooperative control framework based on fuzzy logic, which is specifically designed to maintain a safe distance between vehicles by dynamically integrating braking and lane-change decisions in response to potential hazards. The proposed system aims to improve operational safety and occupant comfort under diverse and complex driving conditions in vehicles.

2.2 Modelling

This study is organized into five sections. First, a dynamic vehicle model with realistic characteristics is presented to enable realistic simulations. Next, we describe the design of the control system responsible for maintaining a safe distance from potential obstacles in the driving environment. The third section presents a trajectory-tracking system that monitors the vehicle's position during evasive maneuvers to ensure stability and a precise response. Furthermore, an obstacle detection system was implemented to identify objects on the road and maintain a safe distance. Finally, the fuzzy logic controllers that comprise the proposed ACC system are described in detail. Figure 1 illustrates the overall system modeling and the interactions between its integrated modules.

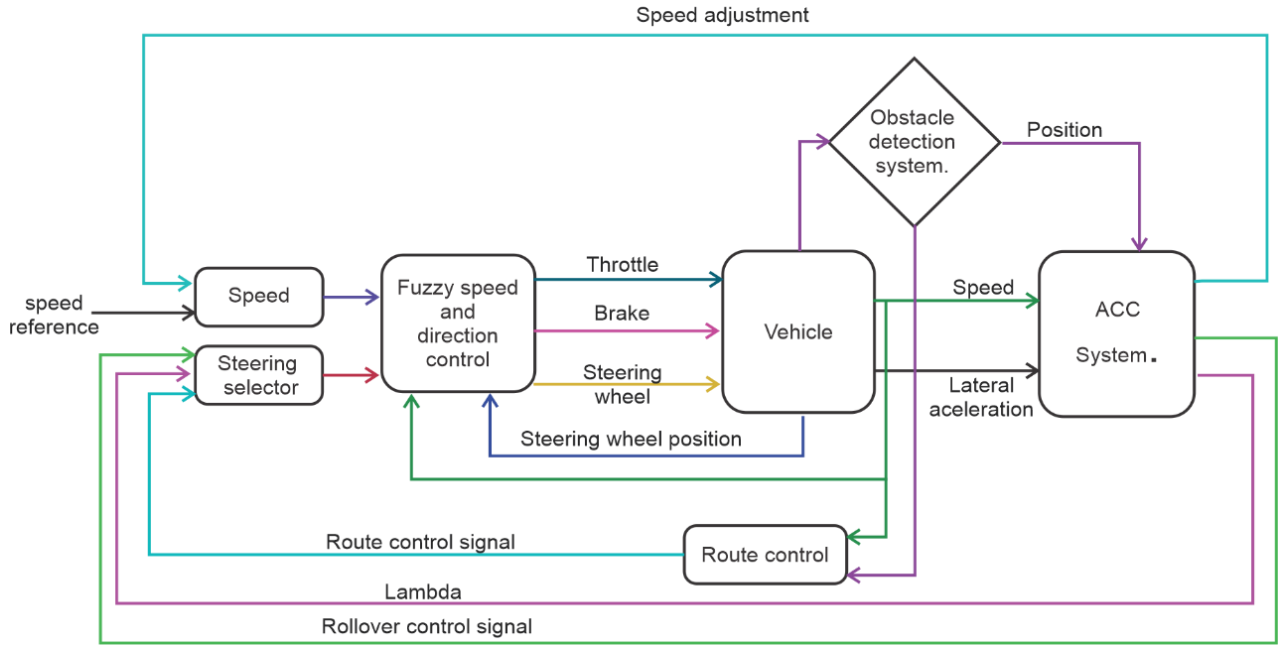


Figure 1. Overall block diagram of the proposed intelligent adaptive cruise control system

2.2.1 Vehicle dynamics

To develop the proposed system, a dynamic model that incorporates the real-world characteristics of a commercial vehicle was used. Table 1 lists the characteristics considered in this model. The goal of the dynamic model was to obtain simulation results that are as representative and as close as possible to real-world behavior. Furthermore, this dynamic model allows for the adjustment of specific parameters to emulate different types of vehicles, thereby increasing its versatility and broadening its applications.

Table 1. Vehicle dynamic model variable

Symbol	Variable
β	Angular position of the center of mass of the vehicle
$\dot{\beta}$	Angular velocity of the center of mass of the vehicle
ψ	Torsion of the vehicle around the vertical axis
M	Vehicle's mass
v	Velocity
F_x	Thrust force
F_a	Aerodynamic force
δ	Turning angle of the tires
F_{yf}	Tangential forces to the front wheel
F_{yt}	Tangential forces to the rear wheel
$\dot{X}$	Vehicle velocity vector
$\dot{Y}$	

The model considers three fundamental variables: the angular velocity $\dot{\beta}$ of the vehicle's center of mass (Eq. (1)), the linear velocity $\dot{v}$ of the center of mass (Eq. (2)), and the vehicle's position on the roadway, determined through the integration of (Eq. (3)). These three variables are used as inputs for the proposed control system, which is responsible for making real-time decisions.

$$\dot{\beta} = \dot{\psi} - \frac{1}{M \cdot v}\left\{\left(\frac{F_x}{2} - F_a\right)\sin(\beta) + \frac{F_x}{2}\sin(\delta + \beta) + F_{yf}\cos(\delta + \beta) + F_{yt}\cos(\beta)\right\} \quad (1)$$

$$\dot{v} = \frac{1}{M}\left\{\frac{F_x}{2}(\cos(\beta) + \cos(\delta + \beta)) - F_a\cos(\beta) - F_{yf}\sin(\delta + \beta) - F_{yr}\sin(\beta)\right\} \quad (2)$$

$$\begin{pmatrix}\dot{X}\\ \dot{Y}\end{pmatrix} = v\begin{pmatrix}\cos(\psi - \beta)\\ \sin(\psi - \beta)\end{pmatrix} \quad (3)$$

2.2.2 Safe distance modeling

As illustrated in Figure 2, each vehicle is characterized by its absolute position (S_H and S_L), velocity (V_H and V_L), and absolute acceleration (a_H and a_L). The relative distance d between the host vehicle and the leading vehicle or obstacle is given as follows:

$$d = S_L - S_H \tag{4}$$

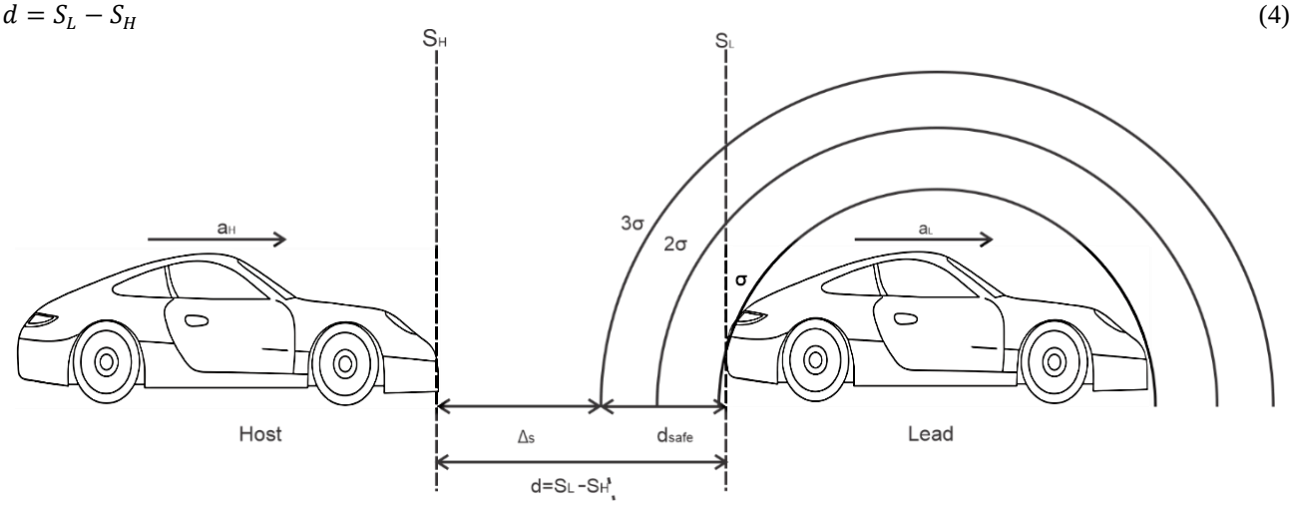


Figure 2. Adaptive cruise control setup

2.2.3 Trajectory tracking system

The control module generates a steering control signal via trajectory tracking. The trajectory error is defined as the angle between the vector representing the desired trajectory and the projection of the line connecting the vehicle's center of mass, located at coordinates $(X, Y)$to a reference point $(100_x, 100_y)$ positioned 100 m ahead along the path. Figure 3 illustrates the geometric relationship used to define this error.

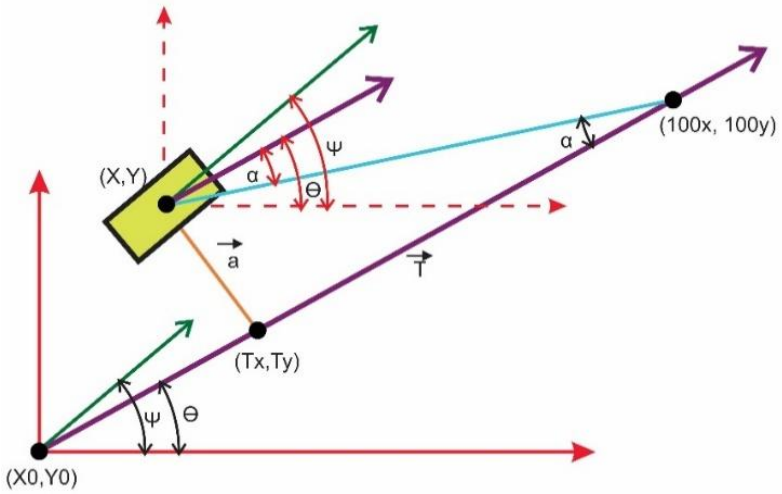


Figure 3. Geometric representation of the trajectory-tracking model used for route control

The origin of the trajectory and the initial steering angle (ψ_0) are known. The orientation angle (ψ), defined by the vehicle's velocity vector, represents the heading of the vehicle relative to the global (X_0) axis. Additionally, (θ) is defined as the slope angle of the planned route with respect to the same (X_0).

2.2.4 Obstacle detection system

A theoretical obstacle detection system based on a multivariable Gaussian distribution function is proposed, representing each obstacle as a circular region with a radius of 3σ. This approach guarantees a high degree of confidence and compliance with the safety distance established in Section 2.2.2, even under conditions of uncertainty. The proposed methods are presented as future alternatives to conventional detection technology, such as LiDAR, which exhibits certain operational limitations such as high implementation costs, sensitivity to adverse weather conditions, and reflection problems [31]. While it is recognized that not all objects can be accurately represented by a Gaussian distribution, the use of an extended safety radius based on 3σ provides a sufficient margin to guarantee collision prevention, even in the presence of uncertainties associated with obstacle detection or characterization. Furthermore, the multivariable Gaussian distribution guarantees that approximately 99.9% of the probability is within a radius of 3σ, thus excluding only a negligible portion of the distribution, as illustrated in Figure 4.

The vehicle is equipped with three sensors, each with a detection range of 100 m. The lateral distance (D_L) is defined as the Euclidean distance (Equation (5)) between the vehicle's center of mass (X, Y) and the center of the circular representation of the obstacle (A_x, A_y), adjusted by subtracting the vehicle's front length (l_f) and the predefined safety margin (3σ).

$$D_L = \sqrt{(A_x - X)^2 + (A_y - Y)^2} - l_f - 3\sigma \tag{5}$$

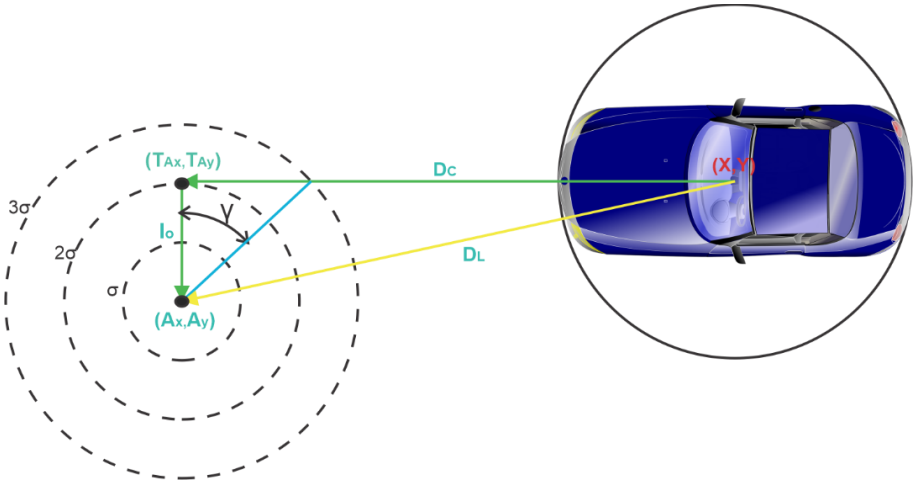


Figure 4. Functional description of the obstacle detection system

A line is defined from the vehicle's center of mass (X, Y) to the center of the obstacle's circular representations (A_x, A_y). From this, a perpendicular segment (l_o) is constructed, extending from the tangency point (T_{Ax}, T_{Ay}) on the circumference to the obstacle center (A_x, A_Y). The critical distance D_C is obtained as shown in Equation (6).

$$D_c = \sqrt{(T_{Ax} - X)^2 + (T_{Ay} - Y)^2} - l_f - 3\sigma * sin(\gamma) \tag{6}$$

where:

$$\gamma = \cos^{-1}\left(\frac{l_o}{3\sigma}\right) \tag{7}$$

The obstacle position (O_p) is defined as follows:

$$O_p = sgn(\overrightarrow{l_o} \times \overrightarrow{D_c}) \tag{8}$$

$$if \quad O_p \geq 0 \rightarrow left$$

$$if \quad O_p < 0 \rightarrow right$$

2.3 Fuzzy ACC with Safety Guarantees

Fuzzy control operates solely on the input and output variables, without requiring an explicit mathematical model of the system. Instead, it relies on linguistic rules that emulate human reasoning and decision-making. This characteristic allows high adaptability and makes it suitable for applications such as autonomous driving, where decisions are made under conditions of uncertainty and imprecise information. In this context, the proposed ACC system employs fuzzy logic to interpret real-time driving conditions, including the speed, acceleration, and position, as well as the speed and location of surrounding obstacles. Based on this information, the system determines appropriate safety maneuvers such as lane changes or emergency braking. Furthermore, it maintains a safe following distance in unpredictable driving scenarios, with obstacle detection acting as a constraint on the minimum permissible distance. The ACC manages acceleration, braking, and steering actions. When an obstacle is detected at a sufficient distance, the controller adjusts the vehicle speed and initiates a lane-change maneuver. Conversely, maximum braking is applied when a collision is imminent. Additionally, the system continuously monitors the lateral acceleration to reduce the risk of rollover and activates a warning signal when critical conditions are detected. All fuzzy controllers were developed using the MATLAB® Fuzzy Logic Toolbox, employing the Mamdani inference mechanism and the centroid defuzzification method.

2.3.1 Fuzzy speed control (throttle and brake)

From a conceptual perspective, human driving involves three hierarchical control levels associated with vehicle acceleration. The first layer is the mechanical layer, which comprises an accelerator pedal and its corresponding hydraulic or mechanical linkages. The second layer is the actuation layer, which is represented by the driver's foot applying a force to the pedal. The third layer is the reasoning layer, which corresponds to the driver's cognitive process and is responsible

for interpreting the surrounding environment and determining the required acceleration. In this study, vehicle behavior is modeled under the assumption of automatic transmission, thereby simplifying the gear-shifting process. Furthermore, the accelerator and brake systems were represented electronically rather than mechanically to reflect the modern drive-by-wire architecture. Accordingly, the proposed control system was organized into three analogous layers. Within this framework, the mechanical layer receives an electrical input signal, which emulates the output of a potentiometer instead of a physical force applied to the accelerator pedal. The electronic layer performs a role analogous to that of the driver's foot by generating a control signal proportional to the desired vehicle speed. The overall structure of the control architecture is illustrated in Figure 5.

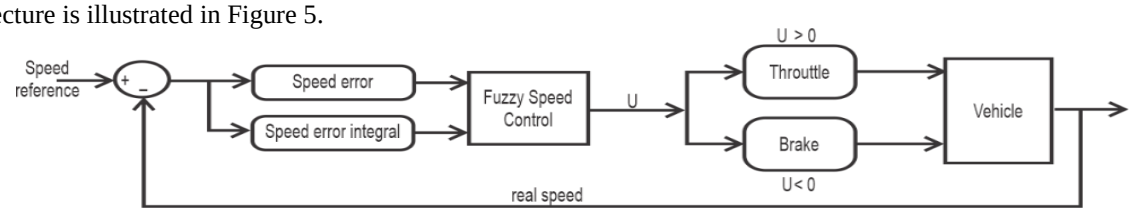


Figure 5. Block diagram of the fuzzy speed controller for throttle and brake actuation

The throttle and brake were considered as a single signal, and positive values were assigned to the throttle and negative values to the brake. When the value of the signal is zero, the null action of the pedals is considered. The inputs to the controller are the velocity error (v_e) and the integral of the velocity error (v_{ei}). These two variables are derived from the reference velocity [km/h], which is defined as the initial condition for the vehicle. The corresponding values are computed using Eqs. (9) and (10).

$$v_e = v_{ref} - v_{real} \tag{9}$$

$$v_{ei} = \int_{t=0}^{T} v_e dt \tag{10}$$

where v_{ref} denotes the velocity reference, v_{real} is the real speed in km/h, and T is the time in seconds.

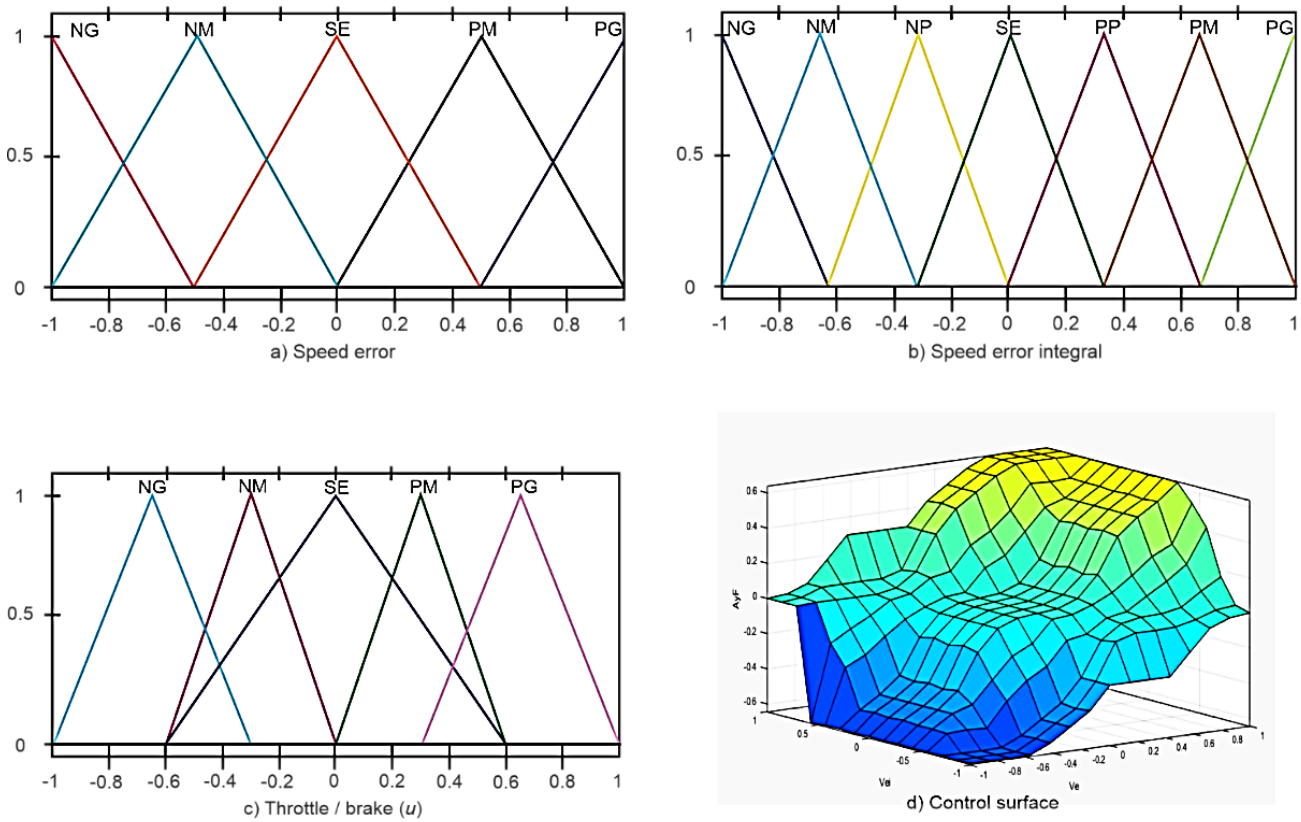


Figure 6. Membership functions and control surface of the fuzzy speed controller: (a) speed-error membership functions; (b) integral-of-speed-error membership functions; (c) throttle/brake output membership functions; and (d) fuzzy control surface

The controller output U, is defined as the percentage of throttle or brake pedal engagement, depending on the sign of the control signal. The proposed fuzzy controller employs five membership functions for both the speed error and controller output (NG, NM, SE, PM, and PG) and seven membership functions for the error integral, incorporating the additional terms NP and PP. To determine the appropriate control action, the output linguistic variables specify whether

throttling (P) or braking (N) should be applied, as well as the magnitude of the action, which is classified as great (G), medium (M), or poor (P). The linguistic term SE represents a neutral condition, in which no control action is applied. As illustrated in Figure 6, the output membership functions were intentionally designed with overlapping regions between SE, NM, and PM. This configuration reduces frequent sign changes in the control signal, thereby preventing continuous switching between throttle and braking actions, which could otherwise result in inefficient and uncomfortable vehicle operation. The controller was based on a rule set consisting of 35 simple fuzzy rules (Table 2) designed to ensure effective speed regulation while emulating human driving behavior.

Table 2. Fuzzy speed control rule summary

		v_{ei}						
		NG	NM	NP	SE	PP	PM	PG
	NG	NG	NG	NG	NG	NG	NM	SE
V_e	NM	NG	NG	NM	NM	NM	SE	PM
	SE	NM	NM	SE	SE	SE	PM	PM
	PM	NM	SE	PM	PM	PM	PG	PG
	PG	SE	PM	PG	PG	PG	PG	PG

2.3.2 Fuzzy steering control (steering wheel)

As in most control systems, the steering controller monitors the error defined as the difference between the reference wheel angle (δ) and the actual measured angle (δ_e), as expressed in Eq. (11). Here, the reference angle (δ_{ref}), represents the desired steering position, whereas the actual angle corresponds to the current steering state, (δ_{real}), and the resulting value is the wheel angle error.

$$\delta_e = \delta_{ref} - \delta_{real} \tag{11}$$

A The second input to the controller is the rate of change of the wheel angle error, calculated according to Eq. (12), which reflects the dynamic behavior of the steering system. The value of $k\ is\ 1/14.7$.

$$\delta_{ed} = \Delta\delta_e = \delta_e(k) - \delta_e(k) \tag{12}$$

Figure 7 illustrates the membership functions used in the fuzzy steering controller. These functions comprise seven linguistic sets: large negative (NL), medium negative (NM), small negative (NS), zero (ZE), small positive (PS), medium positive (PM), and large positive (PL). The complete fuzzy rule base used for decision-making within the controller is listed in Table 3.

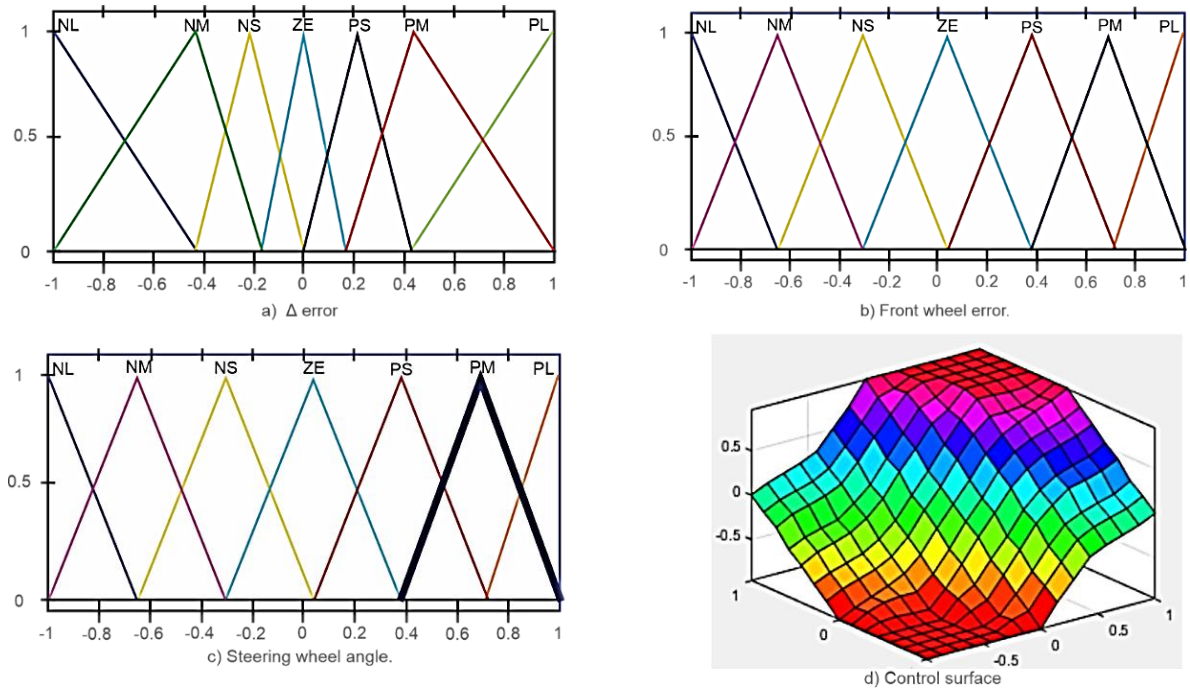


Figure 7. Membership functions and control surface of the fuzzy steering controller: (a) rate-of-change-of-error membership functions; (b) front-wheel-angle-error membership functions; (c) steering-wheel-angle output membership functions; and (d) fuzzy control surface

Table 1. Fuzzy steering control rule summary

		$\Delta\delta_e$						
	ΔU	NL	NM	NS	ZE	PS	PM	PL
	NL	NL	NL	NL	NL	NM	NS	ZE
δ_e	NM	NL	NL	NL	NM	NS	ZE	PS
	NS	NL	NL	NM	NS	ZE	PS	PM
	ZE	NL	NM	NS	ZE	PS	PM	PL
	PS	NM	NS	ZE	PS	PM	PL	PL
	PM	NS	ZE	PS	PM	PL	PL	PL
	PL	ZE	PS	PM	PL	PL	PL	PL

2.3.3 Fuzzy control for collision avoidance

When a potential collision with an object on the road is detected, the vehicle trajectory is redirected to a clear lane or area associated with a more distant obstacle. To facilitate this maneuver, the system evaluates both the proximity of the obstacle and the time-change distance, as defined in Eq. (13). This analysis determines whether an obstacle is approaching, moving away, or stationary relative to the vehicle trajectory. Subsequently, the controller processes the signals provided by each sensor using the current distance (d) and the change from the previous state (Δd). In this formula, t denotes time in seconds.

$$\Delta d = d(t) - d(t-1) \tag{13}$$

The controller utilizes six fuzzy sets as input variables, with each of the three sensors contributing two sets: one representing the measured distance (d) and the other capturing the rate of change in distance over time (Δd). The obstacle distance variables illustrated in Figure 8(a) are defined using four fuzzy sets: risk, near, medium, and far away.

The (Δd) for each zone, depicted in Figure 8(b), consists of three fuzzy sets that describe the relative movement of the obstacle with respect to the autonomous vehicle. These sets indicate whether the distance to the obstacle is increasing $(if\ \Delta d > 0; obstacle\ speed\ (Vm)\ > vehicle\ speed(Va))$, remaining constant $(if\ \Delta d = 0; obstacle\ speed\ (Vm) = vehicle\ speed\ (Va))$, or decreasing $(if\ \Delta d < 0; obstacle\ speed\ (Vm)\ < vehicle\ speed\ (Va))$. A constant or decreasing distance indicates that the obstacle is stationary or traveling at a lower velocity than the vehicle, which consequently increases the risk of collision. The controller output generates the steering wheel displacement required to avoid collisions. As shown in Figure 8(c), the output variable is represented by eight membership functions and expressed in degrees (°). The collision avoidance output comprises a control signal applied directly to the steering system, which modifies the steering wheel angle to perform the required evasive maneuvers. The knowledge base of the controller output is presented in Table 4. The complete set of rules can be found in Appendix A.

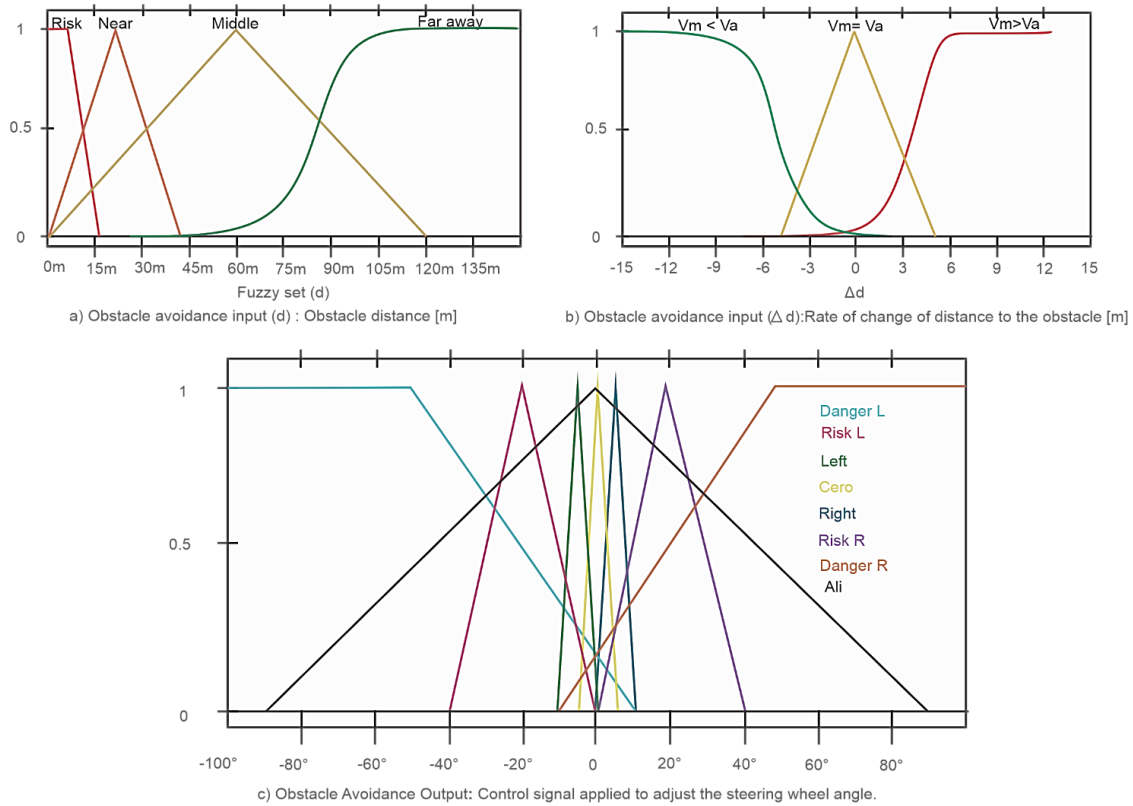


Figure 8. Membership functions of the fuzzy collision-avoidance controller: (a) obstacle-distance input; (b) rate-of-change-of-obstacle-distance input; and (c) steering-angle control output.

Table 4. Knowledge base fuzzy control for collision avoidance

Left sensor (d)	Vm < Va	Vm = Va	Vm > Va
Danger	Danger R	Danger R	Risk R
Near	Danger R	Risk R	Right
Middle	Risk R	Right	Cero
Far away	Right	Cero	Cero

Center sensor (d)	Vm < Va	Vm = Va	Vm > Va
Danger	Danger L	Danger L	Risk L
Near	Danger L	Risk L	Cero
Middle	Left	Cero	Cero
Far away	Cero	Cero	Cero

Right sensor (d)	Vm < Va	Vm = Va	Vm > Va
Danger	Danger L	Danger L	Risk L
Near	Danger L	Risk L	Left
Middle	Risk L	Left	Cero
Far away	Left	Cero	Cero

2.3.4 Fuzzy control for safety distance

The controller evaluates the proximity of the nearest obstacle and determines the corresponding weighting factor for the control signal that is applied to the steering mechanism. It receives three input variables, each of which is associated with a different sensor. The controller output is a dimensionless value ranging from 0 to 1, where 0 indicates that no obstacle has been detected on the road and 1 denotes a high risk of collision. Figures 9(a)–9 (c) show the distance measurements obtained from each sensor, and Figure 9(d) illustrates the relative proximity between the vehicle and the detected obstacle. The sensors operated within a detection range of 0–100 m. The knowledge base (Table 5) was designed to satisfy safety requirements by generating a collision alert whenever an obstacle was detected by any of the sensors. Conversely, the road is considered clear only when at least two sensors indicate the absence of obstacles, prompting the controller to generate the corresponding road-clear signal.

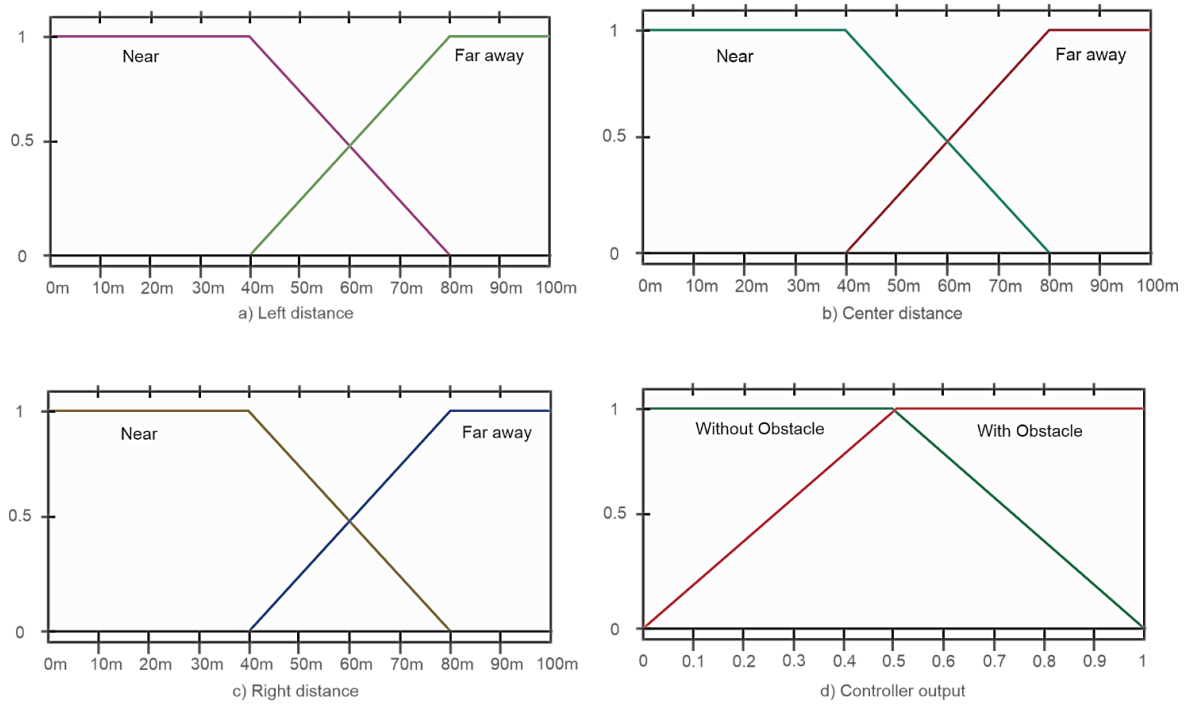


Figure 9. Membership functions of the fuzzy safety-distance controller: (a) left-sensor distance input; (b) centre-sensor distance input; (c) right-sensor distance input; and (d) obstacle-proximity control output

Table 5. Rule summary of fuzzy control for safety distance

If	Obstacle	&	Obstacle		Action
	Far away L		Far away R	→	Low Risk collision
	Far away L		Far away C	→	Low Risk collision
	Far away R		Far away C	→	Low Risk collision
	Near L		-	→	High Risk collision
	Near R		-	→	High Risk collision
	Near C		-	→	High Risk collision

2.3.5 Fuzzy control for speed adjustment

The controller adjusts the throttle signal to reduce the speed of the vehicle and initiates a lane-change maneuver upon obstacle detection to avoid collisions. Once an obstacle is identified, the fuzzy safety-distance controller evaluates the instantaneous velocity of the vehicle. The sensors continuously provide real-time distance measurements of obstacles. The fuzzy controller comprises four fuzzy sets: three inputs and one output. The relative distance set quantifies the collision risk based on obstacle proximity. The real speed set evaluates the vehicle's current speed, enabling the estimation of the minimum deceleration required to safely avoid obstacles, and operates within a maximum range of 50 km/h. Additionally, the speed change set captures the rate at which the obstacle approaches the host vehicle, as defined in Eq. (14).

$$\Delta V = V(t) - V(t-1) \tag{14}$$

where ΔV denotes the change of speed, $V(t)$ is the instant speed, and $V(t-1)$ is the speed in time $(t-1)$.

Finally, the output fuzzy set provides a throttle-adjustment signal to the system. A slope limiter is implemented to prevent sudden increases in the vehicle speed when the host vehicle avoids an obstacle. A summary of the fuzzy rules governing this behavior is provided in Appendix B.

2.3.6 Rollover controller

There is a possibility that the evasive maneuver executed to avoid a collision may expose the vehicle to rollover risk. Rollovers can occur during normal cornering maneuvers on highways. For this reason, the behavior of the lateral acceleration (a_L) was analyzed to evaluate vehicle stability under such conditions.

$$a_L = \frac{V^2}{Radius} \tag{15}$$

where V is the speed of the vehicle and $Radius$ is the radius of the curve.

According to [20], a lateral acceleration of 3 $\mathrm{m/s^2}$ is considered acceptable if the adhesion conditions are adequate. 2 $\mathrm{m/s^2}$ can become almost imperceptible to passengers. However, an acceleration of 4 $\mathrm{m/s^2}$ represents danger, and the vehicle can skid or rollover. Based on Eq. (16), we decided to decrease the longitudinal speed; consequently, the lateral acceleration decreased, as shown in Eq. (15).

$$\Delta a_L = a_L(t) - a_L(t-1) \tag{16}$$

The control system comprises two input variables: the lateral acceleration value provided by the vehicle's dynamic model, and the change in lateral acceleration (Δa_L), as defined in Eq. (16). The lateral acceleration was limited to a maximum of 4 $\mathrm{m/s^2}$indicates an imminent risk of rollover. The objective of this control strategy was to maintain the lateral acceleration at levels imperceptible to passengers, thereby improving ride comfort and safety. The second input acted as a reference signal to evaluate the effectiveness of the speed adjustment control. This indicates whether the lateral acceleration decreases over time, providing feedback on whether speed regulation contributes to enhanced vehicle stability.

2.3.7 Emergency braking control

An emergency braking system addresses the scenario in which an unexpected obstacle appears on the road or where the available distance is insufficient to avoid a collision. The reaction distance (d_r) is defined as the distance traveled by the vehicle between the moment the obstacle is detected and the start of braking as shown in Eq. (17). Moreover, the reaction time (t_r) under normal driving conditions for a young person is generally on average 0.75 s [3]**.** By contrast, the simulation results indicate that the onboard computer system, in conjunction with its corresponding actuator, can achieve a reaction time of approximately 200 ms. However, to incorporate a safety margin in the system's design and evaluation, a conservative reaction time of 0.5 s has been considered.

$$d_r = \frac{v}{3.6} * t_r \tag{17}$$

The braking distance (d_f), defined by Eq. (18), represents the displacement covered by the vehicle after the braking action is initiated. This distance is a function of the vehicle's speed at the exact moment prior to braking(v), as well as the dynamic coefficient of friction (μ) between the tires and the road surface. Finally, the total stopping distance (d_{pt}) is defined as the sum of the reaction and braking distances, as expressed in Eq. (19). The knowledge base for the emergency braking system is presented in Table 6.

$$d_f = \frac{v^2}{2 * g * 3.6^2 * \mu} \tag{18}$$

$$d_{pt} = d_f + d_r \tag{19}$$

Table 6. Knowledge base emergency braking system

$d_{pt} >$	&	$d_{pt} >$		Action
Right Sensor Distance		Centre Sensor Distance	→	Brake
Left Sensor Distance		Centre Sensor Distance	→	Brake

A lateral acceleration (a_L) exceeding 4 m/s^2 is considered hazardous. Because an abrupt deceleration is not advisable in such scenarios, an alarm is triggered to alert the driver or system.

$$\text{if } a_L > \frac{4m}{s^2} \;\&\; \Delta a_L > 0 \rightarrow \text{alarm is activated}$$

2.3.8 Speed adjustment selection

In this control algorithm, two signals are considered for vehicle speed adjustment: one generated by the speed adjustment controller and the other generated by the rollover prevention controller. Accordingly, a prioritization criterion was established to determine which signal should take precedence based on the current driving conditions. To enhance safety, the control system always selects a signal corresponding to the greatest speed reduction, thereby addressing the most critical risk. Additionally, the speed reduction does not exceed the current speed of the vehicle.

2.3.9 Steering adjustment selection

The steering of the vehicle is governed by two control signals: one generated by the route tracking controller and the other by the fuzzy collision avoidance controller. Relative weighting factors are assigned to each signal according to the obstacle distance using a safe distance control signal (DS) as a reference. Subsequently, a sigmoid function is applied to dynamically adjust these weighting factors, prioritizing the collision avoidance signal as the vehicle approaches the obstacle and favoring the route tracking signal when the obstacle is located at a greater distance. The steering system receives the control signal corresponding to the controller with the highest weighting factor (λ), as defined in Eq. (20).

$$\lambda = \frac{1}{1 + e^{-15(DS-0.5)}} \tag{20}$$

$$applied\ signal = S_{S.T.}(\lambda - 1) + S_{P.C.}(\lambda) \tag{21}$$

where $S_{S.T.}$ is the route control signal and $S_{P.C.}$ is the fuzzy control for the collision avoidance signal. An explanation of the sigmoid function is beyond the scope of this study. Finally, the integration and interaction of all fuzzy controllers described in this section are illustrated in Figure 10. The simulation block diagram illustrates the overall architecture and operational flow of the control system, and describes the interactions among the vehicle model, sensor inputs, fuzzy controllers, and actuator outputs.

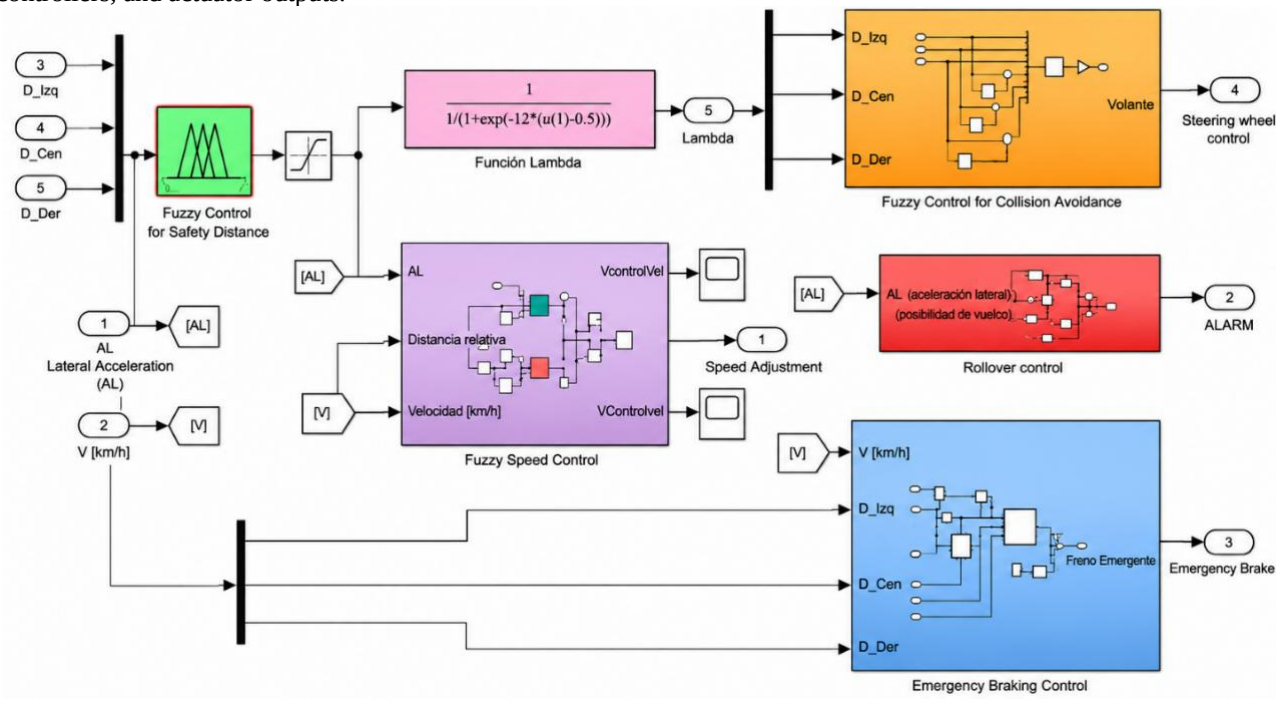


Figure 10. MATLAB/Simulink implementation of the proposed fuzzy logic-based intelligent adaptive cruise control architecture

3. Results and Discussion

To validate the results, a dynamic model with real parameters emulating a 2010 Volkswagen® Tiguan was implemented. The validation process began by verifying the model's consistency and performance, followed by evaluating its response to obstacle scenarios in the MATLAB® Simulink environment. For the validation procedure, data were acquired from the vehicle's four corners, center of mass, and velocity vector. These tests confirmed that the model maintained stable motion without abrupt changes in position, direction, or rotation along the vertical, longitudinal, and transverse axes. Figure 11 shows the simulated vehicle, where the velocity vector is represented in green, vehicle outline in blue, and center of mass in black. The acceleration and brake pedal behaviors were validated using actual pressure data. The

pressure applied to an actual vehicle was replicated in the simulation environment to compare the resulting speeds. Figure 12 shows the results of the four tests, demonstrating good agreement between the simulated and real speeds, although deviations of up to 15 km/h were observed at specific time instants. Table 7 presents the quantitative analysis, where the mean absolute error did not exceed 3 km/h (less than 3.5%), and the root mean square error was 3.95 km/h (4.6%). All tests were performed under identical initial conditions. These results confirm that the dynamic model accurately reproduced the behavior of the vehicle.

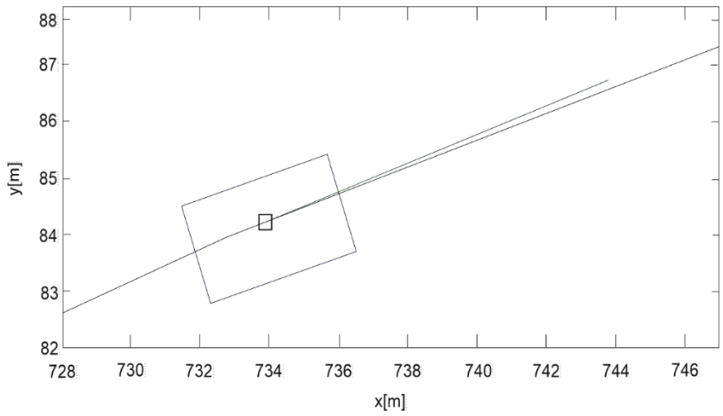


Figure 11. Validation tests of the dynamic model's kinematic behavior

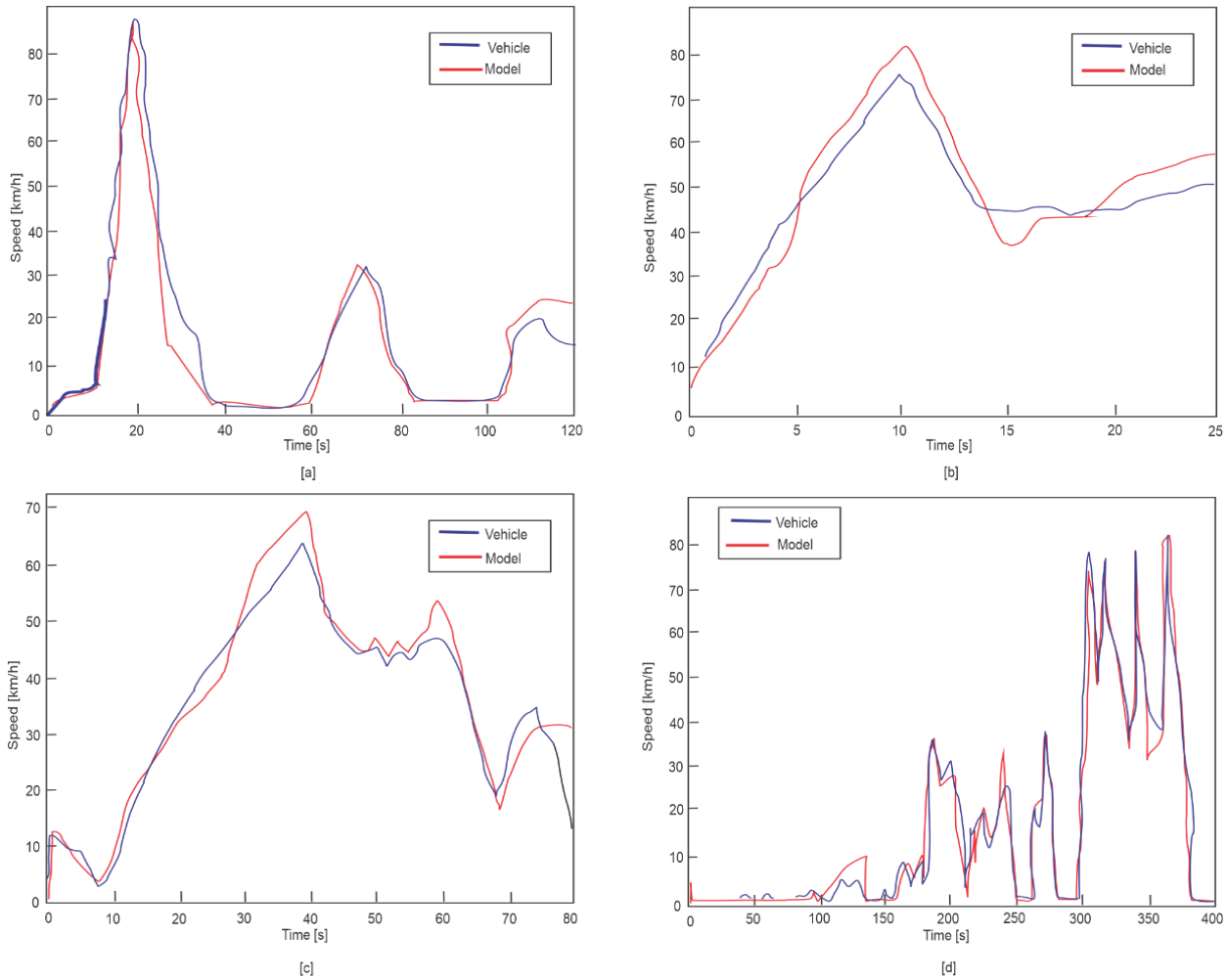


Figure 12. Validation tests for the dynamic model's speed

Table 7. Throttle validation results

	Test a)	Test b)	Test c)	Test d)	Overall, MAE	[Units]
Mean Absolute Error	2.51	5.32	2.38	1.73	2.99	[km/h]
Maximum Speed	85.93	85.89	63.00	69.00	85.93	[km/h]
% Mean Error	2.92	6.19	3.78	2.51	3.47	[%]
Maximum Error	15.92	9.07	12.00	14.24	15.92	[km/h]
% Maximum Error	18.53	10.56	19.04	20.64	18.53	[%]
Root Mean Square Error	4.06	5.87	3.11	2.76	3.95	[km/h]
% Root Mean Square Error	4.73	6.83	4.93	4.00	4.60	[%]

The system response was evaluated using three scenarios in which obstacles of varying sizes were placed along the vehicle, representing the size of a pedestrian or small vehicle. In the second scenario, a similarly sized obstacle was placed on the right side, representing another vehicle. Finally, a large obstacle comparable in size to a house was placed directly in front of the vehicle to evaluate the system under extreme conditions. Obstacles were placed at different distances to assess the reaction time of the system. The test results are presented in Figures 13(a-c). In these figures, the vehicle path is shown in magenta, and the obstacles are represented by red circles. The three safety radii used by the object detection system to maintain a safe distance are also presented. The figures illustrate the lane-change maneuver performed to avoid collisions, as well as the total distance required for the vehicle to return to its original path. The test conditions are listed in Table 8. The simulation tests yielded satisfactory results, with the system avoiding collisions in 99% of the evaluated cases. This high success rate is attributed to the strict adherence to the defined safety ratio, positioning the proposed system as a promising alternative to existing less effective approaches.

However, in some scenarios, the lane-change maneuver proved to be suboptimal because of the large distance required for its execution. This limitation is expected to be mitigated under real conditions where road limits would restrict lane changes, causing the obstacle detection system to inhibit such maneuvers when they are not feasible. While the use of the tree radius is effective in avoiding collisions, it increases the space required for evasive action. This presents a challenge for future work: optimizing or reducing the radius to allow for more efficient lane changes without compromising safety. The system demonstrated stability in returning to the original trajectory after encountering small obstacles, as shown in Figure 13(a), and medium-sized obstacles such as other vehicles (Figure 13(b)). However, when larger deviations were introduced, as shown in Figure 13(c), the vehicle exhibited instability, resulting in a delay in returning to its initial trajectory. This highlights an area of improvement for future development.

Table 8. Summary of test conditions

Test Conditions	Test 1	Test 2	Test 3
Obstacle position	X=500 m Y = -1.5 m	X=600 m Y = 1m	X = 200 m Y = 0.5 m
Obstacle size	0.3 m	2 m	10 m
Speed host vehicle	35 km/h	35 km/h	35 km/h

An additional key aspect is the analysis of the vehicle speed behavior, as illustrated in Figures 14(a) and 14(b). These figures show the reference speed in magenta, actual vehicle speed in blue, and the speed correction applied by the proposed ACC system. The results indicate satisfactory tracking of the reference speed with smooth transitions and no overshoot, ensuring passenger comfort. Furthermore, the vehicle responded appropriately to the speed adjustments provided by the ACC, demonstrating effective and stable performance. The tests conducted to evaluate the effectiveness of the anti-rollover system designed to anticipate skidding and rollover scenarios yielded valuable results. The implementation of this control significantly enhances safety by gradually reducing the speed of the vehicle to a level that poses no risk to passengers.

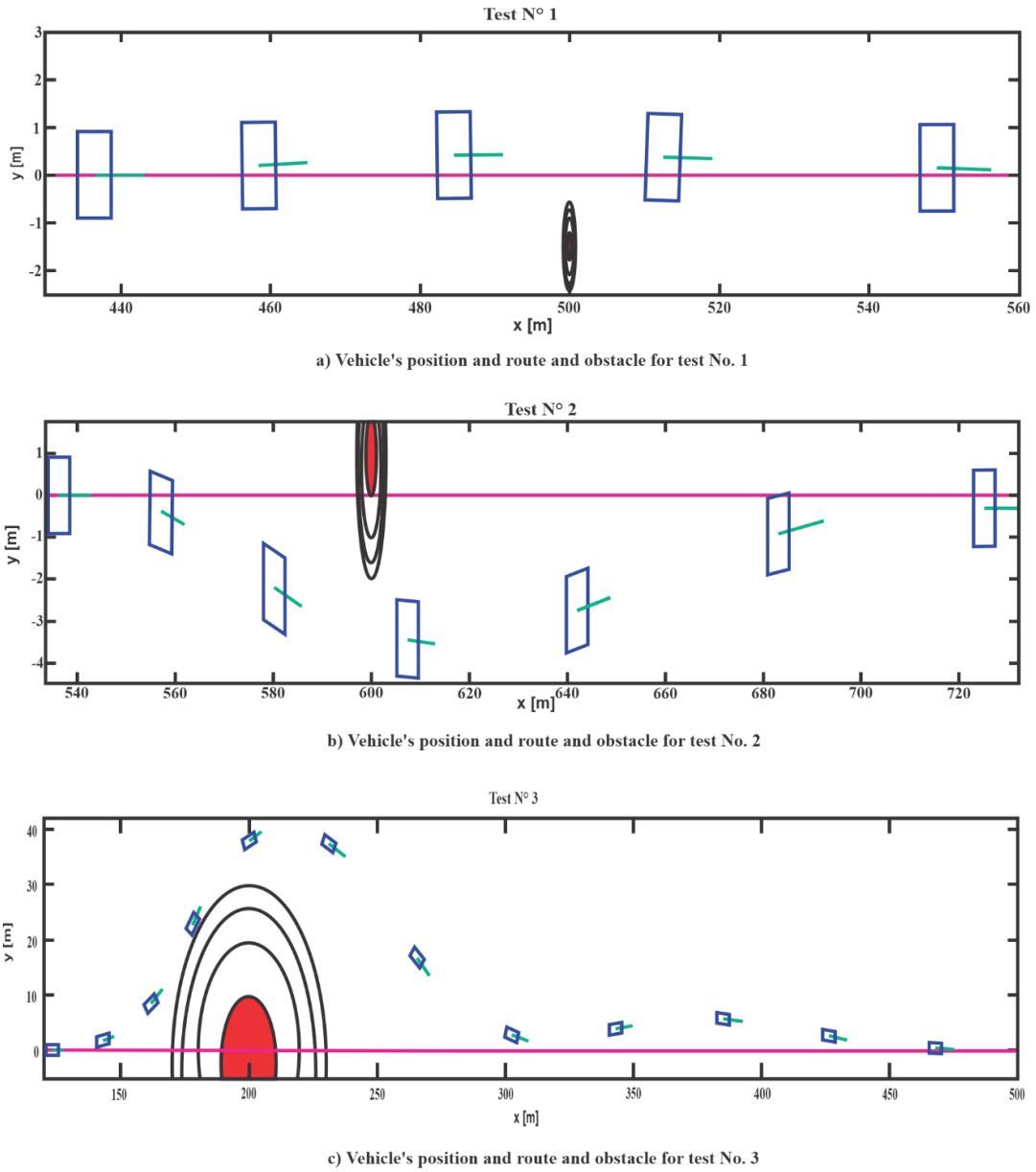


Figure 13. Vehicle trajectories during the collision-avoidance tests for different obstacle configurations: (a) Test No. 1, small obstacle; (b) Test No. 2, medium-sized obstacle; and (c) Test No. 3, large obstacle

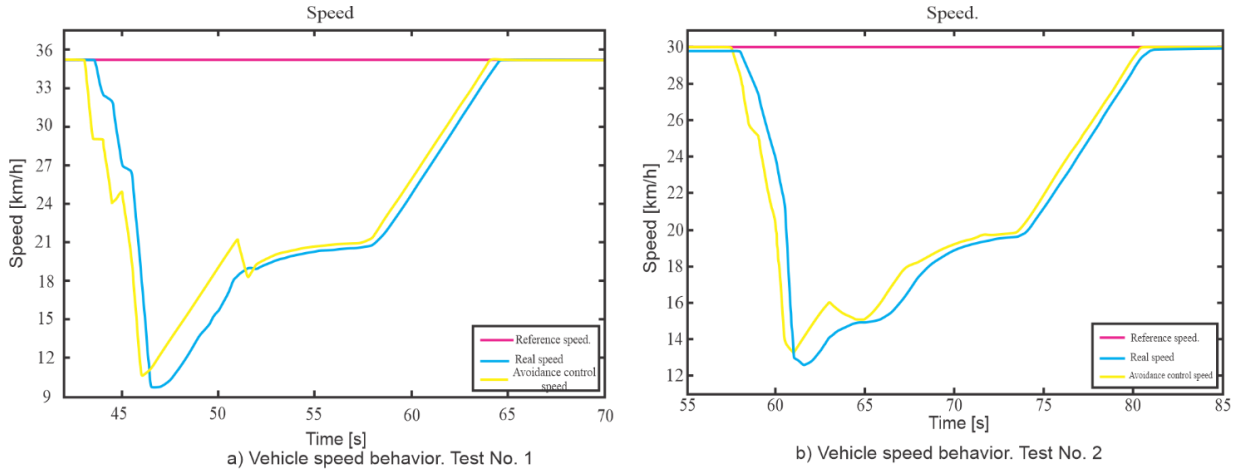


Figure 14. Vehicle speed response during collision-avoidance manoeuvres: (a) reference and actual vehicle speeds; and (b) speed adjustment generated by the proposed ACC system

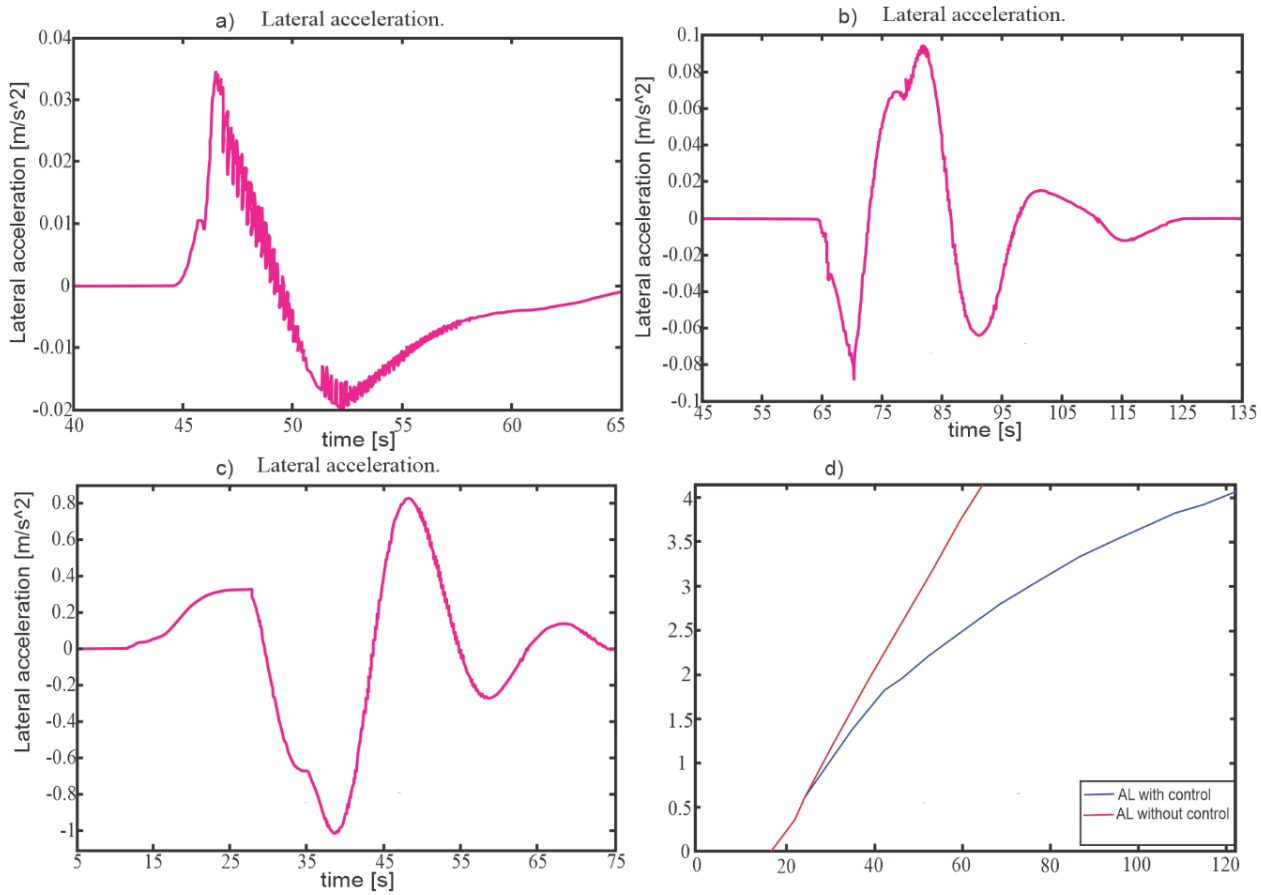


Figure 15. Lateral acceleration for a) Test No. 1, b) Test No. 2, c) Test No. 3 and d) vehicle comparison with and without lateral acceleration control

Rollover control was triggered when the lateral acceleration reached an initial threshold of 0.5 m/s^2. In the first two tests, which involved standard maneuvers, the maximum lateral acceleration remained below 0.1 m/s2, as shown in Figures 15(a) and 15(b). The variation in lateral acceleration is defined according to Eq. (16), and under these conditions, the rollover control remained inactive. In contrast, the third test, shown in Figure 15(c), presented a lateral acceleration variation exceeding 0.2 m/s, activating the rollover control. This activation was also reflected in the speed profile of the vehicle. Additionally, the steering input was excessive relative to the instantaneous speed of the vehicle, which exceeded 26 km/h, producing a lateral acceleration that, although not hazardous, was perceptible to passengers and may affect comfort. Finally, Figure 15(d) shows the behavior of the lateral acceleration with and without rollover control, thus demonstrating that with rollover control, it is possible to prolong a vehicle's travel. The implementation of an emergency braking system is a fundamental safety feature. This ensures the protection of both the vehicle and passengers in situations in which it is impossible to avoid a sudden obstacle, react to a sudden stop by the vehicle ahead, or maneuver around an obstruction. The results obtained during emergency braking scenarios, such as the sudden appearance of an obstacle or inability to perform a lane change, were acceptable. However, the data also revealed that an effective braking response required a longer braking distance than the current safety radius. Conventional ACC systems often exhibit delayed responses in emergency situations; therefore, the proposed approach, with further improvements, offers a promising solution to this limitation.

4. Conclusions

This study presented an IACC system based on fuzzy logic for collision avoidance in autonomous vehicles. The proposed architecture integrates obstacle detection, longitudinal speed control, lateral steering control, rollover prevention, and emergency braking into a unified decision-making framework capable of selecting the safest maneuver based on the driving scenario. The simulation results demonstrated that the proposed controller avoided collisions in 99.9% of the evaluated scenarios, representing the main contribution of this study. The fuzzy controller generated smooth lane changes when sufficient space was available and activated emergency braking when it was not possible to avoid obstacles by steering alone. Furthermore, lateral acceleration monitoring contributes to maintaining vehicle stability and improving passenger comfort during evasive maneuvers. While the proposed system showed satisfactory performance in realistic MATLAB® Simulink simulations, future work will focus on experimental validation with real vehicles, sensor fusion with LiDAR, radar and cameras, and testing in more complex traffic and environmental conditions to improve the robustness and applicability of the proposed system.

Acknowledgements
The author expresses gratitude to the Secretaría de Ciencia, Humanidades, Tecnología e Innovación (SECIHTI). Special thanks to the Istituto Politécnico Nacional (IPN).

Declaration of Competing Interests
The authors affirm that they have no competing interests regarding this work.

CRediT Author Contribution Statement
J.C. Suárez-Calderón: Methodology; Writing-original draft; Conceptualization; Model Verification
I. Rocha-Gómez: Data Curation; Visualisation; Writing-review
O. Susarrey-Huerta: Writing-review; Data Curation; Supervision
D. Desiderio-Maya: Writing-review and editing; Data Curation; Visualisation

Ethics Statement
This study did not involve human participants or animal subjects. Therefore, this research did not require ethical approval.

Generative Artificial Intelligence Declarations
The authors claim that artificially intelligent-assisted technologies, such as generative AI, were not used to generate content, ideas, or theories. We have used AI to enhance readability and refine the language. This was done with extreme human control and oversight. The authors take full responsibility for reviewing and approving the content.

References
[1] W. Wu, D. Zou, J. Ou, and L. Hu, "Adaptive cruise control strategy design with optimized active braking control algorithm," *Mathematic Problems Engineering*, vol. 2020, no. 1, p. 8382734, 2020, https://doi.org/10.1155/2020/8382734.
[2] N. C. Basjaruddin, Kuspriyanto, D. Saefudin, and I. K. Nugraha, "Developing adaptive cruise control based on fuzzy logic using hardware simulation," *International Journal of Electrical and Computer Engineering*, vol. 4, no. 6, pp. 944-951, 2014, https://doi.org/10.11591/ijece.v4i6.6734.
[3] G. O. Burnham, J. Seo, and G. A. Bekey, "Identification of human driver models in car following," *IEEE transactions on Automatic Control*, vol. 19, no. 6, pp. 911-915, 1974, https://doi.org/10.1109/TAC.1974.1100740.
[4] J. E. Naranjo, C. Gonzaález, J. Reviejo, R. Garciía, and T. de Pedro, "Adaptive fuzzy control for inter-vehicle gap keeping," *IEEE Transactions on Intelligent Transportation Systems*, vol. 4, no. 3, pp. 132-142, 2003, https://doi.org/10.1109/TITS.2003.821294.
[5] J. J. Martinez and C. Canudas-de-Wit, "A safe longitudinal control for adaptive cruise control and stop-and-go scenarios," *IEEE Transactions on Control Systems Technology*, vol. 15, no. 2, pp. 246-258, 2007, https://doi.org/10.1109/TCST.2006.886432.
[6] T. Stanger and L. Del Re, "A model predictive cooperative adaptive cruise control approach," in *Proceedings of the American Control Conference*, 2013, pp. 1374-1379. https://doi.org/10.1109/acc.2013.6580028.
[7] C. Piao, J. Gao, Q. Yang, and J. Shi, "Adaptive cruise control method based on hierarchical control and multi-objective optimization," *Transactions of the Institute of Measurement and Control*, vol. 45, no. 7, pp. 1298-1312, 2023, https://doi.org/10.1177/01423312221137508.
[8] J. Chen, F. Tao, Z. Fu, and N. Wang, "Vehicle-following control based on continuous synthesis variable time headway model," *International Journal of Fuzzy Systems*, vol. 27, no. 3, pp. 912-930, 2025, https://doi.org/10.1007/s40815-024-01814-z.
[9] S. Abdallaoui, H. Ikaouassen, A. Kribèche, A. Chaibet, and E. Aglzim, "Advancing autonomous vehicle control systems: An in-depth overview of decision-making and manoeuvre execution state of the art," *The Journal of Engineering*, vol. 2023, no. 11, Art. no. e12333, 2023, https://doi.org/10.1049/tje2.12333.
[10] F. Kamil, F. H. Gburi, M. A. Kadhom, and B. A. Kalaf, "Fuzzy logic-based control for intelligent vehicles: A survey," in *AIP Conference Proceedings*, 2024, vol. 3092, no. 1, Art. no. 040017, https://doi.org/10.1063/5.0199602.
[11] R. Li, S. Deng, and Y. Hu, "Autonomous vehicle modeling and velocity control based on decomposed fuzzy PID," *International Journal of Fuzzy Systems*, vol. 24, no. 5, pp. 2354-2362, 2022, https://doi.org/10.1007/s40815-022-01279-y.
[12] H. Ekanayake, P. Abejeewa, W. A. L. Priyankara, and A. Induranga, "Overview of use of PID, fuzzy logic, and model predictive control in autonomous vehicle systems," *International Journal of Research and Scientific Innovation*, vol. 12, no. 10, pp. 3685-3697, 2025, https://doi.org/10.51244/ijrsi.2025.1210000318.
[13] N. Awad, A. Lasheen, M. Elnaggar, and A. Kamel, "Model predictive control with fuzzy logic switching for path tracking of autonomous vehicles," *ISA transactions*, vol. 129, pp. 193-205, 2022, https://doi.org/10.1016/j.isatra.2021.12.022.
[14] S. Hao, Y. Chen, J. Gao, H. He, and Y. Wang, "Fuzzy model predictive control for collision avoidance control of autonomous vehicles," in *Advances in Transdisciplinary Engineering*, 2025, pp. 267-277, https://doi.org/10.3233/ATDE250427.

[15] I. Aliskan, "The optimization-based fuzzy logic controllers for autonomous ground vehicle path tracking," *Engineering Applications of Artificial Intelligence*, vol. 151, Art. no. 110642, 2025, https://doi.org/10.1016/j.engappai.2025.110642.
[16] Ambuj and R. Machavaram, "Intelligent path planning for autonomous ground vehicles in dynamic environments utilizing adaptive Neuro-Fuzzy control," *Engineering Applications of Artificial Intelligence*, vol. 144, Art. no. 110119, 2025, https://doi.org/10.1016/j.engappai.2025.110119.
[17] W. Medina Medina, "Diseño de un sistema de control de tráiler autónomo," *Ingeniería Industrial*, pp. 25-66, 2022, https://doi.org/10.26439/ing.ind2022.n.5799.
[18] B. Suprapto and S. Dwijayanti, "Comparative performance of fuzzy logic and PID steering control for improved swerve autonomous vehicles," *Jurnal RESTI (Rekayasa Sistem dan Teknologi Informasi)*, vol. 10, pp. 516–527, 2026, https://doi.org/10.29207/resti.v10i2.7594.
[19] B. Wang, Y. Lei, Y. Fu, and X. Geng, "Autonomous vehicle trajectory tracking lateral control based on the terminal sliding mode control with radial basis function neural network and fuzzy logic algorithm," *Mechanical Sciences*, vol. 13, no. 2, pp. 713-724, 2022, https://doi.org/10.5194/ms-13-713-2022.
[20] B. Arifin, B. Y. Suprapto, S. A. D. Prasetyowati, and Z. Nawawi, "Steering control in electric power steering autonomous vehicle using type-2 fuzzy logic control and PI control," *World Electric Vehicle Journal*, vol. 13, no. 3, p. 53, 2022, https://doi.org/10.3390/wevj13030053.
[21] B. Y. Suprapto, S. Dwijayanti, and M. I. Fadillah, "Design and optimization of a type-2 fuzzy logic-based lateral control system for enhancing trajectory stability in autonomous vehicles," *Eastern-European Journal of Enterprise Technologies*, vol. 3, no. 3, Art. no. 86, 2025, https://doi.org/10.15587/1729-4061.2025.326193.
[22] S Devikala, "Development of fuzzy logic controller in automatic vehicle navigation using IoT," *Journal of Electrical Systems*, vol. 20, no. 3s, pp. 114-121, 2024, https://doi.org/10.52783/jes.1254.
[23] S. Jain and I. Malhotra, "A fuzzy logic design for self-driving vehicle to avoid obstacles," in *Uncertainty in Computational Intelligence-Based Decision Making: A volume in Advanced Studies in Complex Systems*, pp. 143-171, 2024, https://doi.org/10.1016/B978-0-443-21475-2.00015-1.
[24] Q. Liu, Z. Song, X. Xu, J. Wang, and J. P. Lazaro, "Research on vehicle obstacle avoidance control based on improved artificial potential field method and fuzzy model predictive control," *Vehicles*, vol. 8, no. 4, p. 86, 2026, https://doi.org/10.3390/vehicles8040086.
[25] L. Wang, X. Deng, J. Gui, and S. Wan, "Fuzzy logic-based probabilistic forecasting of short-term trajectory for autonomous vehicles," *IEEE Transactions on Consumer Electronics*, vol. 71, no. 2, pp. 7158-7169, 2025, https://doi.org/10.1109/TCE.2025.3541570.
[26] M. Sadaf, Z. Iqbal, Z. Anwar, U. Noor, M. Imran, and T. R. Gadekallu, "A novel framework for detection and prevention of denial of service attacks on autonomous vehicles using fuzzy logic," *Vehicular Communications*, vol. 46, Art. no. 100741, 2024, https://doi.org/10.1016/j.vehcom.2024.100741.
[27] S. Nahavandi, S. Mohamed, I. Hossain, et al., "Autonomous convoying: A survey on current research and development," *IEEE Access*, vol. 10, pp. 13663-13683, 2022, https://doi.org/10.1109/ACCESS.2022.3147251.
[28] S. Magdici and M. Althoff, "Adaptive cruise control with safety guarantees for autonomous vehicles," in *IFAC-PapersOnLine*, vol. 50, no. 1, pp. 5774-5781, 2017. https://doi.org/10.1016/j.ifacol.2017.08.418.
[29] K. W. Schmidt, "Cooperative adaptive cruise control for vehicle following during lane changes," vol. 50, no. 1, pp. 12582-12587, 2017. https://doi.org/10.1016/j.ifacol.2017.08.2199.
[30] A. Ondoğan and H. S. Yavuz, "Fuzzy logic based adaptive cruise control for low-speed following," in *2019 3rd International Symposium on Multidisciplinary Studies and Innovative Technologies (ISMSIT)*, 2019, pp. 1-5, https://doi.org/10.1109/ISMSIT.2019.8932776.
[31] M. U. Khan, S. A. A. Zaidi, A. Ishtiaq, S. U. R. Bukhari, S. Samer, and A. Farman, "A comparative survey of LiDAR-SLAM and LiDAR based sensor technologies," in *Proceedings of the 2021 Mohammad Ali Jinnah University International Conference on Computing, MAJICC 2021*, 2021, pp. 1-8, https://doi.org/10.1109/MAJICC53071.2021.9526266.

Appendix

Appendix A. Fuzzy control for collision avoidance, rule summary

If	Left Zone.	&	(**Δd**) Left		Action
	danger		Vm<Va	→	danger - right.
	danger		Vm=Va	→	danger - right.
	danger		Vm>Va	→	risk - right.
	near		Vm<Va	→	danger - right
	near		Vm=Va	→	risk - right
	near		Vm>Va	→	right
	middle		Vm<Va	→	risk - right.
	middle		Vm=Va	→	right
	middle		Vm>Va	→	Cero.
	far away		Vm<Va	→	right
	far away		Vm=Va	→	Cero.
	far away		Vm>Va	→	Cero.
If	Center Zone.	&	(Δd) Center		Action.
	danger		Vm<Va	→	danger - left
	danger		Vm=Va	→	danger - left
	danger		Vm>Va	→	risk - left
	near		Vm<Va	→	danger - left
	near		Vm=Va	→	risk - left
	near		Vm>Va	→	Cero.
	middle		Vm<Va	→	left
	middle		Vm=Va	→	Cero.
	middle		Vm>Va	→	Ali.
	far away		Vm<Va	→	Ali.
	far away		Vm=Va	→	Ali.
	far away		Vm>Va	→	Ali.
If	Right Zone.	&	(Δd) Right.		Action.
	danger		Vm<Va	→	danger - left
	danger		Vm=Va	→	danger - left.
	danger		Vm>Va	→	risk - left
	near		Vm<Va	→	danger - left
	near		Vm=Va	→	risk - left
	near		Vm>Va	→	left
	middle		Vm<Va	→	risk - left
	middle		Vm=Va	→	left
	middle		Vm>Va	→	Cero.
	far away		Vm<Va	→	left
	far away		Vm=Va	→	Cero.
	far away		Vm>Va	→	Cero.

Appendix B. Fuzzy control for speed adjustment. Rule summary

If	Distance	&	Speed	&	→	Action
	near		slow	$\Delta v \gg 0$	→	RF
	near		middle	$\Delta v \gg 0$	→	RF
	near		fast	$\Delta v \gg 0$	→	RMF
	middle		slow	$\Delta v \gg 0$	→	RA
	middle		middle	$\Delta v \gg 0$	→	RF
	middle		fast	$\Delta v \gg 0$	→	RF
	far away		slow	$\Delta v \gg 0$	→	RB
	far away		middle	$\Delta v \gg 0$	→	RA
	far away		fast	$\Delta v \gg 0$	→	RF
	near		slow	$\Delta v \geq 0$	→	RA
	near		middle	$\Delta v \geq 0$	→	RF
	near		fast	$\Delta v \geq 0$	→	RF
	middle		slow	$\Delta v \geq 0$	→	RB
	middle		middle	$\Delta v \geq 0$	→	RB
	middle		fast	$\Delta v \geq 0$	→	RF
	far away		slow	$\Delta v \geq 0$	→	RMB
	far away		middle	$\Delta v \geq 0$	→	RB
	far away		fast	$\Delta v \geq 0$	→	RA
	near		slow	$\Delta v \leq 0$	→	RA
	near		middle	$\Delta v \leq 0$	→	RA
	near		fast	$\Delta v \leq 0$	→	RF
	middle		slow	$\Delta v \leq 0$	→	RB
	middle		middle	$\Delta v \leq 0$	→	RB
	middle		fast	$\Delta v \leq 0$	→	RA
	far away		slow	$\Delta v \leq 0$	→	RN
	far away		middle	$\Delta v \leq 0$	→	RMB
	far away		fast	$\Delta v \leq 0$	→	RB
	near		slow	$\Delta v \ll 0$	→	RB
	near		middle	$\Delta v \ll 0$	→	RA
	near		fast	$\Delta v \ll 0$	→	RA
	middle		slow	$\Delta v \ll 0$	→	RMB
	middle		middle	$\Delta v \ll 0$	→	RB
	middle		fast	$\Delta v \ll 0$	→	RA
	far away		slow	$\Delta v \ll 0$	→	RN
	far away		middle	$\Delta v \ll 0$	→	RN
	far away		fast	$\Delta v \ll 0$	→	RMB
	No risk		-	-	→	RN